Science of the Total Environment 615 (2018) 1–8

Contents lists available at ScienceDirect

Science of the Total Environment

journal homepage: www.elsevier.com/locate/scitotenv

Contribution of forests to the carbon sink via biologically-mediated silicate weathering: A case study of China

Zhaoliang Song [a,*], Hongyan Liu [b,*], Caroline A.E. Strömberg [c,*], Hailong Wang [d], Peter James Strong [e], Xiaomin Yang [a], Yuntao Wu [a]

[a] Institute of the Surface-Earth System Science Research, Tianjin University, Tianjin 300072, China
[b] College of Urban and Environmental Sciences, Peking University, Peking 100871, China
[c] Department of Biology, Burke Museum of Natural History and Culture, University of Washington, Seattle, WA 98195, USA
[d] School of Environmental and Chemical Engineering, Foshan University, Foshan, Guangdong 528000, China
[e] School of Chemistry, Physics and Mechanical Engineering, Queensland University of Technology, GPO Box 2432, 2 George St, Brisbane, QLD 4001, Australia

HIGHLIGHTS

- Atmospheric CO_2 sequestration through weathering is a stable carbon sink.
- Plants biologically enhance weathering-related CO_2 consumption.
- Biomass-related silicate weathering in China may consume 7.9 ± 4.1 Tg CO_2 yr^{-1}.
- Forests may increase CO_2 sequestration through silicate weathering by ~32%.

GRAPHICAL ABSTRACT

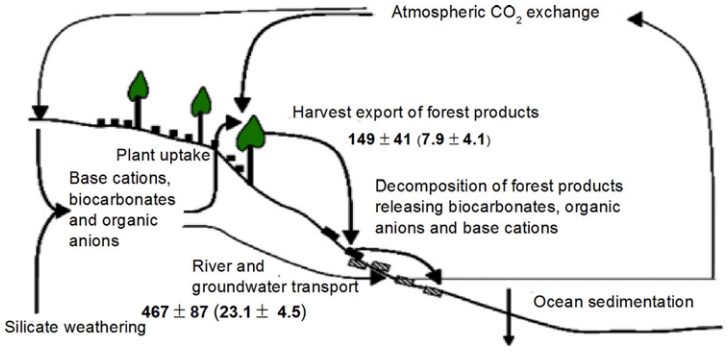
Atmospheric CO2 exchange
Harvest export of forest products
149 ± 41 (7.9 ± 4.1)
Plant uptake
Base cations, biocarbonates and organic anions
Decomposition of forest products releasing biocarbonates, organic anions and base cations
River and groundwater transport
467 ± 87 (23.1 ± 4.5)
Ocean sedimentation
Silicate weathering

ARTICLE INFO

Article history:
Received 20 July 2017
Received in revised form 22 September 2017
Accepted 23 September 2017
Available online 29 September 2017

Editor: Elena Paoletti

Keywords:
Enhanced-silicate weathering
CO_2 consumption
Forest
Bamboo
China

ABSTRACT

During silicate weathering, atmospheric carbon dioxide (CO_2) is consumed and base cations are released from silicate minerals to form carbonate and bicarbonate ions, which are finally deposited as carbonate complexes. Continental silicate weathering constitutes a stable carbon sink that is an important influence on long-term climate change, as it sequesters atmospheric carbon dioxide at a million-year time scale. Traditionally, CO_2 sequestered through silicate weathering is estimated by measuring the flux of the base cations to watersheds. However, plants also absorb considerable amounts of base cations. Plant biomass is often removed from ecosystems during harvesting. The base cations are subsequently released after decomposition of the harvested plant materials, and thereby enhance CO_2 consumption related to weathering. Here, we analyze plant biomass storage-harvest fluxes (production and removal of biomass from forests) of base cations in forests across China to quantify the relative contribution of forest trees to the terrestrial weathering-related carbon sink. Our data suggest that the potential CO_2 consumption rate for biomass-related silicate weathering (from the combined action of with afforestation/reforestation, controlled harvesting and rock powder amendment) in Chinese forests is 7.9 ± 4.1 Tg CO_2 yr^{-1}. This represents ~34% of the chemical weathering rate in China. Globally, forests may increase CO_2 sequestration through biologically-mediated silicate weathering by ~32%.

© 2017 Elsevier B.V. All rights reserved.

* Corresponding authors at: Institute of the Surface-Earth System Science Research, Tianjin University, NO. 92, Weijin Road, Tianjin 300072, China.
E-mail addresses: zhaoliang.song@tju.edu.cn (Z. Song), lhy@urban.pku.edu.cn (H. Liu), caestrom@u.washington.edu (C.A.E. Strömberg).

https://doi.org/10.1016/j.scitotenv.2017.09.253
0048-9697/© 2017 Elsevier B.V. All rights reserved.

1. Introduction

During silicate weathering, atmospheric carbon dioxide (CO_2) is consumed and base cations are released from silicate minerals to form carbonate and bicarbonate ions, which are finally deposited within soil profiles or transported to a lake or marine environment and precipitated as carbonate complexes (Gaillardet et al., 1999; Amiotte-Suchet et al., 2003; Song et al., 2012). Each year, the chemical weathering of continental silicates consumes 380 to 553 Mt (or Tg) of atmospheric carbon dioxide globally (Meybeck, 1987; Gaillardet et al., 1999). Despite this major contribution to the global carbon sink, the role of chemical weathering in the terrestrial carbon balance and in climate change has until recently only been considered in studies dealing with geological time scales as it was thought to be a relatively slow process (e.g. Berner, 1997; Gaillardet et al., 1999; Hagedorn and Cartwright, 2009; Maher and Chamberlain, 2014). However, recent data analyses and modeling have indicated (1) that continental silicate weathering flux responds to 10 to 100 year-scale climate change (Gislason et al., 2009; Beaulieu et al., 2012), and (2) that the flux may be greatly accelerated by rapid erosion (Larsen et al., 2014), the addition of pulverized silicate rocks to soils and sea (Schuiling and Krijgsman, 2006; Köhler et al., 2010; Cressey, 2014; Moosdorf et al., 2014; Taylor et al., 2016), or terrestrial plant growth (Berner, 1997; Moulton et al., 2000; Song et al., 2011; Manning and Renforth, 2012). As an example of the latter, the sequestration flux of atmospheric CO_2 through weathering of Icelandic basalts correlates directly with wetland coverage and net primary production (NPP) (Kardjilov et al., 2006).

In addition to acid generation to release nutrients for biomass generation and microbial-induced chelation (Drever, 1994; Taylor et al., 2009; Manning and Renforth, 2012; Manning et al., 2013), an important mechanism underlying the silicate weathering caused by plants is the rapid uptake of base cations and silicon during plant growth and harvest (Balogh-Brunstad et al., 2008). This removal destabilizes silicate minerals (Bormann et al., 1998; Song et al., 2012; Vadeboncoeur et al., 2014). It has recently been estimated that changes in silica (SiO_2), potassium (K), sodium (Na), calcium (Ca) and magnesium (Mg) uptake by terrestrial vegetation may significantly affect silicate weathering on time scales as short as 100 to 1000 years (Street-Perrott and Barker, 2008; Uhlig et al., 2017). The effect of plants on continental silicate weathering caused by nutrient uptake varies greatly among different vegetation types (Street-Perrott and Barker, 2008; Song et al., 2011, 2012) and is influenced by growth phases of vegetation and the timing of harvest (Balogh-Brunstad et al., 2008). Generally, the nutrient uptake effect of forests on weathering is thought to surpass that of other terrestrial ecosystems (e.g. grasslands, wetlands and croplands) due to a greater plant biomass storage-harvest flux (the flux in kg ha^{-1} yr^{-1}) and lower fluxes of fertilizer application (Street-Perrott and Barker, 2008; Song et al., 2011).

Both carbon and base cations are sequestered during wood production and released after wood degradation/oxidation (Bormann et al., 1998; Vadeboncoeur et al., 2014). A significant amount of base cations absorbed by forest plants is removed from forests during biomass harvesting. These are often released elsewhere after decomposition of the harvested forest products, although the release time of cations from lumber products depends on the processing and use of the timber (Bormann et al., 1998; Sverdrup and Rosen, 1998; Vadeboncoeur et al., 2014). Base cations and bicarbonates derived from direct silicate weathering (Gaillardet et al., 1999; Amiotte-Suchet et al., 2003; Song et al., 2012) and released from decomposed forest material may finally be deposited at the bottom of a soil profile, or transported to a lake or marine environment and precipitated as carbonates. Therefore, forest plant growth and harvesting may enhance biological weathering-related CO_2 consumption (Song et al., 2012). However, the precise contribution made by forests to the continental silicate weathering carbon sink has not been quantified at a regional or a global scale.

Here, we evaluate the impact of forests on rates of continental-weathering related carbon sequestration using China as a case study. China accounts for 6% of the global CO_2 consumption rate related to weathering (Qiu et al., 2004; Wu et al., 2011) and has $>140 \times 10^6$ ha of forests growing on soils dominated by silicate minerals. Most of the forests in China are distributed in subtropical and temperate hilly or mountainous areas - with sufficient primary silicate mineral generated from soil erosion and disturbed by human activities such as harvesting (Fang et al., 2001; FAO, 2010). Although repeated intensive forest harvesting may finally exhaust soil base cation pool as a result of biomass harvest removal and base cation leaching loss (Lucas et al., 2014), we hypothesize that combination with other measures such as silicate rock powder amendment in some forest regions with extremely acidic soils, sustainable harvest of forests such as those in China can accelerate silicate weathering and supply base cations for forest regeneration (Bormann et al., 1998; Vadeboncoeur et al., 2014). We use the mass balance calculation method based on data of forest area, average cation contents of trees weighted by tissue biomass, and NPP of forests (Materials and methods section) to compare CO_2 consumption flux and rates of biomass-related silicate weathering among different forest types and to investigate the contribution of forests to carbon sink through continental silicate weathering.

2. Materials and methods

2.1. General characteristics of the Chinese forests

Chinese forests range from tropical forests in the south to boreal forests in the north. To better understand the silicate weathering carbon sink in Chinese forests, we divided Chinese forests developed on soils dominated by silicate minerals into seven forest types based on climatic conditions and physiology: tropical (T) forest, subtropical and tropical bamboo (STB) forest, subtropical evergreen broad-leaf and mixed (SEBM) forest, subtropical and tropical coniferous (STC) forest, temperate deciduous broad-leaf (TDB) forest, coniferous and broad-leaf mixed

Table 1
Characteristics of the seven Chinese forest types (Hou, 1982; Song et al., 2013).

Forest type[a]	Area (10^6 ha)	MAP (mm)[b]	MAT (°C)[c]	Forest subtype
T	0.95	1600–2000	21–26	Semi-deciduous monsoon forest, Montane rainforest
STB	7.2	1000–2000	14–26	*Phyllostachys pubescens* forest, *Phyllostachys violascens* forest
SEBM	33.9	800–1600	16–20	*Castanopsis* forest, *Pinus-Castanopsis* mixed forest, *Lithocarpus xylocarpus* forest
STC	29.5	800–1600	8–20	*Cunninghamia lanceolata* forest, *Cathaya argyrophylla* forest, *Pinus massoniana* forest, *Pinus armandii* forest
TDB	42.4	500–1000	8–20	*Quercus variabilis* forest, *Quercus liaotungensis* forest, *Quercus mongolica* forest, *Betula platyphylla* forest
CB	4.7	500–1600	2–14	*Pinus-Quercus* mixed forest, Broad leaf tree-*Pinus* mixed forest
CTC	24.1	400–600	−6–8	*Pinus tabulaeformis* forest, *Platycladus orientalis* forest, *Pinus koraiensis* forest, *Pinus sylvestris* var.*mongolica* forest, *Larix gmelinii* forest

[a] T, tropical forest; STB, subtropical and tropical bamboo forest, SEBM, subtropical evergreen broad-leaf and mixed forest; STC, subtropical and tropical coniferous forest; TDB, temperate deciduous broad-leaf forest; CB, coniferous and broad-leaf mixed forest; CTC, cold-temperate and temperate coniferous forest.
[b] MAP, mean annual precipitation.
[c] MAT, mean annual temperature.

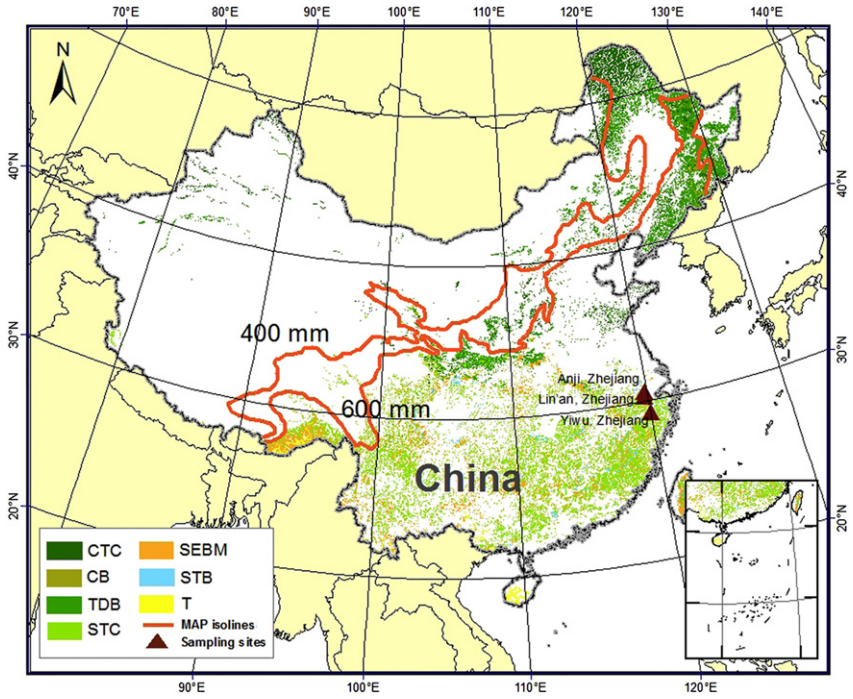

Fig. 1. Distribution of the seven forest types in China and sampling sites.

(CB) forest, and cold-temperate and temperate coniferous (CTC) forest. The plant composition and other characteristics vary greatly among the forest types (Table 1, Fig. 1).

In China, the bedrock of forests is primarily composed of granite and basalt. Approximately 60% of the forested area is located in mountainous area, and has an altitude higher than 500 m and a slope > 10 degrees. The erosion in mountainous areas in China is intense to mild (Wang et al., 2011; Zhang et al., 2014; Ma et al., 2016) and most of the weathering regimes (>60%) of the forests in China are not kinetically limited. The depth of the forest soils exceeds 5 m in the tropical areas, but is <1 m in the cold-temperate areas. The degree of weathering and age of the soils follow similar trends. As most soils are acidic, forests from relatively flat areas with a soil depth exceeding 2 m may benefit from rock powder amendment that enhance silicate weathering.

2.2. Collection of forest tree biomass, NPP, and elemental composition data

For all forest types but STB, forest tree biomass, NPP, and elemental composition data were obtained from published monographs (Chen

Table 2
Tissue biomass-weighted average contents of cations ($C_{i,\ tree}$) in trees of the seven Chinese forest types.

Forest type	Forest subtype	Average contents of cations (g kg^{-1})								Data sources
		Na		K		Ca		Mg		
		Mean	SD	Mean	SD	Mean	SD	Mean	SD	
T	Semi-deciduous monsoon forest	–	–	2.39	–	1.06	–	0.69	–	Chen et al., 1997
	Montane rain forest	–	–	0.89	–	0.35	–	0.35	–	Chen et al., 1997
STB	*Phyllostachys pubescens* forest	0.26	0.05	4.05	0.93	0.70	0.39	0.36	0.05	This study; Huang et al., 2013
	Phyllostachys praecox forest	0.30	0.02	5.05	0.34	0.98	0.07	0.92	0.03	This study; Huang et al., 2013
SEBM	*Castanopsis* forest	–	–	3.24	0.97	2.43	0.87	1.16	0.22	Chen et al., 1997
	Pinus-Castanopsis mixed forest	–	–	2.02	0.53	1.74	0.46	0.79	0.19	Chen et al., 1997
	Lithocarpus xylocarpus forest	–	–	2.41	0.39	3.99	1.28	0.61	0.10	Chen et al., 1997
STC	*Cunninghamia lanceolata* forest	–	–	1.57	0.26	2.63	0.49	0.71	0.13	Chen et al., 1997
	Pinus massoniana forest	–	–	0.81	0.09	1.05	0.04	0.43	0.16	Chen et al., 1997
	Pinus armandii forest	–	–	2.34	–	2.28	–	0.55	–	Chen et al., 1997
TDB	*Quercus variabilis* forest	–	–	2.13	–	10.40	–	0.61	–	Chen et al., 1997
	Quercus liaotungensis forest	–	–	1.97	–	17.73	–	0.74	–	Chen et al., 1997
	Quercus mongolica forest	–	–	2.70	–	8.60	–	0.57	–	Chen et al., 1997
	Betula platyphylla forest	–	–	1.99	–	9.41	–	0.73	–	Chen et al., 1997
CB	*Pinus-Quercus* mixed forest	–	–	2.62	0.23	10.67	2.93	0.91	0.15	Chen et al., 1997
	Broad leaf tree- *Pinus* mixed forest	–	–	2.69	–	5.77	–	0.42	–	Chen et al., 1997
CTC	*Pinus tabulaeformis* forest	–	–	1.97	0.51	2.19	0.31	0.46	0.13	Chen et al., 1997
	Platycladus orientalis forest	–	–	3.01	–	10.53	–	0.51	–	Chen et al., 1997
	Pinus koraiensis forest	–	–	1.14	0.31	1.78	0.97	0.51	0.16	Chen et al., 1997
	Pinus sylvestris forest	–	–	0.88	–	2.01	–	0.84	–	Chen et al., 1997
	Larix gmelinii forest	–	–	1.73	0.27	3.68	1.12	0.47	0.19	Chen et al., 1997

"–" represents lack of data in the reference.

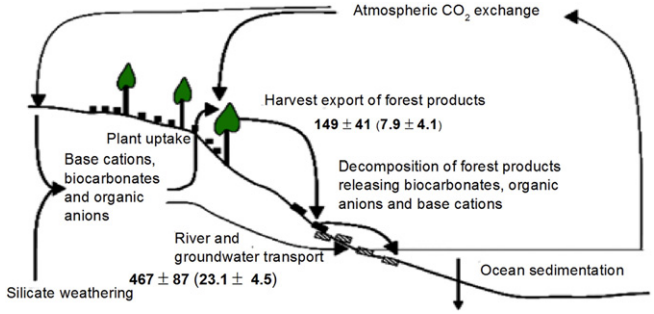
Atmospheric CO_2 exchange
Harvest export of forest products
149 ± 41 (7.9 ± 4.1)
Plant uptake
Base cations, biocarbonates and organic anions
Decomposition of forest products releasing biocarbonates, organic anions and base cations
River and groundwater transport
467 ± 87 (23.1 ± 4.5)
Ocean sedimentation
Silicate weathering

Fig. 2. Mechanisms of CO_2 consumption from biomass-related silicate weathering at a millennial time scale. Biomass-related silicate weathering is related with forest harvest, which creates a new route of biogeochemical cycles of base cations, biocarbonates and organic anions through harvest of forest products in forests and then decomposition of forest products in other places such as coastal plains. The numbers before parenthesis represent global CO_2 consumption rates and their standard deviations. The numbers within parenthesis represent CO_2 consumption rates and their standard deviations in China.

et al., 1997; Feng et al., 1999), and journal articles (Tang et al., 2003; Li and Ren, 2004; Katagiri et al., 2005; Huang et al., 2013).

2.3. Sampling and analysis of plant tissues (STB forest type)

Moso bamboo (*Phyllostachys pubescens*) forests in Lin'an, Zhejiang, and Lei bamboo (*Phyllostachys violascens*) forests in Yiwu, Zhejiang used in this study were developed on granitic hills with slopes exceeding 10 degrees. The soils of the two forests were acidic and deeper than 2 m. The erosion of the soils was moderate.

We collected mature plant tissue samples including leaves, branches, stems, roots, and rhizomes (whip shoots) with three replicates for each plant tissue type from the moso bamboo forests and the Lei bamboo forests in August 2011 (Fig. 1). Each plant tissue sample comprised approximately 300 g of composite plant matter. The sampling procedure matched the other data sources listed in Table 2. The tissue samples were cleaned, oven dried at 75 °C, weighed and crushed. They were fused with Li-metaborate at 1000 °C, dissolved with dilute nitric acid (HNO_3), and analyzed for their K, Na, Ca and Mg contents using inductively coupled plasma-optical emission spectroscopy (ICP-OES). Monitoring with standard samples (GSV-1) and repetition analysis allowed for precision that was better than 5%. The results are shown in Table 2.

2.4. Estimation of the biomass-related silicate weathering carbon sink

Atmospheric CO_2 consumption rate of biomass-related silicate weathering ($R_{CO_2\ \text{consumption,BSW}}$ in 10^{-3} Tg CO_2 yr^{-1} or 10^9 g CO_2 yr^{-1}) can be estimated as:

$$R_{CO_2\ \text{consumption,BSW}} = F_{CO_2\ \text{consumption,BSW}} \times A_k \quad (1)$$

where $F_{CO_2\ \text{consumption,BSW}}$ (in kg CO_2 ha^{-1} yr^{-1}) is CO_2 consumption flux of biomass-related silicate weathering and A_k is the area of a region k (in 10^6 ha).

At a geological time scale (millions of years), only Ca- and Mg- silicate weathering will lead to carbonate precipitation in soil profiles, lakes or the ocean that release 1 mol of CO_2 for 2 mol of CO_2 consumed (Fig. S1) (Gaillardet et al., 1999). However, at a millennial scale, all silicate weathering (including that enhanced by plant harvesting) will sequester CO_2, because the base cations and bicarbonates released from biomass decomposition may also be finally precipitated as carbonates. The inorganic carbon sequestered can be finally derived from atmosphere through photosynthesis (Fig. 2) (Moulton et al., 2000; Song et al., 2012; Manning et al., 2013). $F_{CO_2\ \text{consumption,BSW}}$ can be calculated as (modified from Moulton et al., 2000; Hagedorn and Cartwright, 2009):

$$F_{CO_2\ \text{consumption,BSW}} = (2 \times F_{Ca,BSW}/40 + 2 \times F_{Mg,BSW}/24 + F_{K,BSW}/39 + F_{Na,BSW}/23) \times 44 \quad (2)$$

where $F_{Ca,BSW}$, $F_{Mg,BSW}$ and $F_{K,BSW}$ are forest storage-harvest flux of Ca, Mg and K, respectively, from biomass-related silicate weathering.

Table 3
Biomass storage-harvest flux ($F_{biomass,FBSH}$) and net storage-harvest fluxes of some cations ($F_{i,FESW}$) (i = K, Ca, Mg) in Chinese forests.

Forest type	Forest subtype	Biomass storage-harvest flux (t ha^{-1} yr^{-1})[a]		Net storage-harvest fluxes of cations (kg ha^{-1} yr^{-1})[b]					
				K		Ca		Mg	
		Mean	SD	Mean	SD	Mean	SD	Mean	SD
T	Semi-deciduous monsoon forest	11.18	5.90	26.74	14.11	11.82	6.24	7.68	4.05
	Montane rain forest	7.44	1.55	6.61	1.38	2.63	0.55	2.59	0.54
STB	*Phyllostachys pubescens* forest	9.75	4.03	39.53	25.40	6.81	6.63	3.52	1.92
	Phyllostachys praecox forest	7.26	3.47	36.71	19.99	7.10	3.91	6.71	3.42
SEBM	*Castanopsis* forest	7.67	3.20	24.85	17.82	18.60	14.41	8.86	5.38
	Pinus-Castanopsis mixed forest	4.99	2.05	10.10	6.80	8.68	5.84	3.95	2.57
	Lithocarpus xylocarpus forest	9.04	2.86	21.76	10.41	36.08	22.98	5.52	2.62
STC	*Cunninghamia lanceolata* forest	4.58	2.06	7.19	4.41	12.05	7.69	3.23	2.03
	Pinus massoniana forest	2.31	0.90	1.87	0.94	2.44	1.05	0.99	0.76
	Pinus armandii forest	1.58	0.46	3.70	1.08	3.61	1.06	0.88	0.26
TDB	*Quercus variabilis* forest	2.22	0.46	4.73	0.99	23.12	4.82	1.35	0.28
	Quercus liaotungensis forest	2.04	0.43	4.02	0.84	36.25	7.55	1.51	0.32
	Quercus mongolica forest	1.48	0.57	4.00	1.55	12.72	4.94	0.85	0.33
	Betula platyphylla forest	2.57	1.61	5.10	3.20	24.15	15.15	1.87	1.17
CB	*Pinus-Quercus* mixed forest	1.11	0.23	2.90	0.86	11.80	5.70	1.00	0.38
	Broad leaf tree- *Pinus* mixed forest	3.37	1.05	9.06	2.82	19.42	6.04	1.41	0.44
CTC	*Pinus tabulaeformis* forest	3.27	1.69	6.44	4.98	7.15	4.70	1.51	1.19
	Platycladus orientalis forest	0.50	0.11	1.52	0.32	5.31	1.11	0.26	0.05
	Pinus koraiensis forest	2.01	0.42	2.30	1.11	3.57	2.70	1.02	0.54
	Pinus sylvestris var. *mongolica* forest	1.41	0.46	1.24	0.40	2.84	0.92	1.19	0.38
	Larix gmelinii forest	3.17	1.54	5.48	3.52	11.68	9.22	1.50	1.34

[a] Biomass storage-harvest flux was estimated using Eq. (4) with data on average NPP in all forest types but STB taken from the literature (Tang et al., 2003; Li and Ren, 2004; Katagiri et al., 2005; Huang et al., 2013; Pan et al., 2011).
[b] $F_{i,BSW}$ was estimated with Eq. (3). The flux of Na was not directly shown in this table because of not enough original Na content data.

Although data regarding the Na content in most tree tissues is not available, available data from pine and bamboo forests indicate that the molar ratio of Na/K in tree tissues is approximately 0.1 (Katagiri et al., 2005; data from this study). Thus, for forests without Na data, the Na flux can be estimated by assuming 10% of the K flux.

Forest biomass storage-harvest flux ($F_{\text{biomass,FBSH}}$, t ha^{-1} yr^{-1}) and tissue biomass weighted content of cation i in trees ($C_{i,\text{tree}}$, g kg^{-1}) (Table 2) can be used to estimate $F_{i,\text{BSW}}$ (i = Ca, Mg, K and Na, kg ha^{-1} yr^{-1}) (Table 3):

$$F_{i,\text{BSW}} = F_{\text{biomass,FBSH}} \times C_{i,\text{tree}} \quad (3)$$

Average net primary production in forest j (NPP_j, t ha^{-1} yr^{-1}) (Chen et al., 1997; Feng et al., 1999) and biomass harvest potential percentage of storage in forest j (K_j, %) can be used to estimate $F_{\text{biomass,FBSH}}$ (Table 3):

$$F_{\text{biomass, FBSH}} = \text{NPP}_j \times \text{K}_j \quad (4)$$

where K_j represents a sustainable biomass harvest percentage of storage without compromising purposes of forest conservation and maximizing NPP, and varies with forest management practices. As the total percentage of planted forests and forests with clearly visible anthropogenic activity in China (~90%) is much higher than in the world (~70%) (Fang et al., 2001; FAO, 2010; Pan et al., 2011), forests in China are more frequently harvested than in the whole world for sustainable forest production and commercial purposes. Based on forest management practices in China (Chen et al., 1997; Feng et al., 1999) and the world (Vitousek et al., 1986; FAO, 2010), the potential K_j values were taken as 40 ± 10% and 30 ± 10% for Chinese forests and world's forests, respectively.

3. Results

3.1. CO_2 consumption of silicate weathering in different forests of China

Our analysis shows that the total potential CO_2 consumption rate for biomass-related silicate weathering in Chinese forests is 7.9 ± 4.1 Tg CO_2 yr^{-1}, approximately 39% and 34% of which is due to SEBM and TDB forests, respectively (Fig. 3a). The corresponding CO_2 consumption flux of biomass-related silicate weathering in Chinese forests varies from 20 kg CO_2 ha^{-1} yr^{-1} to 100 kg CO_2 ha^{-1} yr^{-1}, with an area weighted average of 56 kg CO_2 ha^{-1} yr^{-1} (Fig. 3b). This CO_2 consumption flux is significantly higher in angiosperm-dominated forest types, in particular subtropical and tropical bamboo forest (STB) and SEBM than that in other forests. High CO_2 consumption fluxes combined with extensive forested areas are responsible for the higher contribution of SEBM and TDB in total CO_2 consumption rate compared to other Chinese forest types (Fig. 3a, b).

3.2. Spatial differences of CO_2 consumption from silicate weathering

The CO_2 consumption rate from biomass-related silicate weathering is geographically heterogeneous, with the main contributions from southwestern China, eastern China, and central southern China (Fig. 4a–f). In these regions with high CO_2 consumption rate (Fig. 4c–e), the elevated CO_2 consumption flux levels of SEBM, rather than the area of the respective region, are mainly responsible for the large CO_2 sequestering rates (Fig. 4a–f).

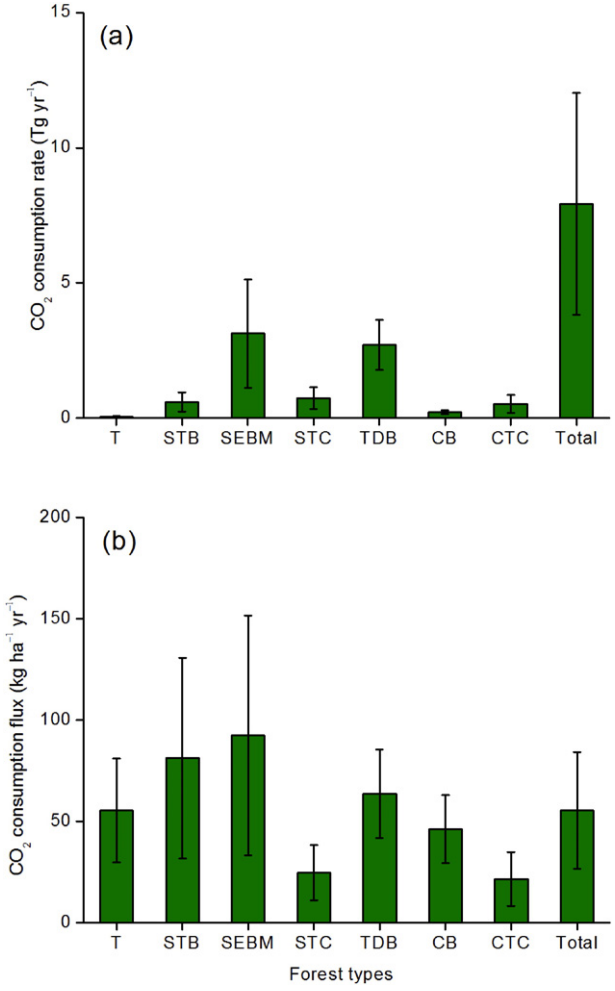

Fig. 3. CO_2 consumption rate ($R_{CO_2\ \text{consumption,BSW}}$, Tg CO_2 yr^{-1}) (a) and flux ($F_{CO_2\ \text{consumption,BSW}}$, kg CO_2 ha^{-1} yr^{-1}) (b) of biomass-related silicate weathering in forest of China. T, tropical forest; STB, subtropical and tropical bamboo forest; SEBM, subtropical evergreen broad-leaf and mixed forest; STC, subtropical and tropical coniferous forest; TDB, temperate deciduous broad-leaf forest; CB, coniferous and broad-leaf mixed forest; CTC, cold-temperate and temperate coniferous forest. *Total* = the total rate or average flux of CO_2 consumption due to biomass-related weathering in Chinese forests. The thin vertical bars represent standard deviations. For details on calculation of CO_2 consumption rate and flux see Materials and methods section.

4. Discussion

4.1. Factors controlling CO_2 consumption of silicate weathering in forests

Silicate weathering rates and fluxes in fast-growing, frequently-harvested forests such as bamboo are closely related to the rate of biomass growth and the frequency and time of harvest (Balogh-Brunstad et al., 2008). The significant correlation between CO_2 consumption flux and biomass storage-harvest flux (Fig. 5) suggests that forest biomass production and removal play a central role in regulating CO_2 sequestration in Chinese forests. This indicates that the high CO_2 consumption flux of biomass-related silicate weathering in wet and warm subtropical and tropical climatic conditions is mainly controlled by rapid tree growth coupled with substantial forest harvesting. This occurs in STB and SEBM forests (Fig. 3b) and regions of southwestern China, eastern China, and central southern China (Fig. 6). Changes in forest management practices (e.g. afforestation/reforestation) in these forests and regions could therefore strongly impact China's total rate of CO_2 consumption.

4.2. Contribution of forests to silicate weathering at a national and global scale

It is difficult to directly compare weathering fluxes calculated using different methods (Futter et al., 2012). Nonetheless, our study indicates that the CO_2 consumption from biomass-related silicate weathering in forests may approximate 35% of weathering in traditional basalt

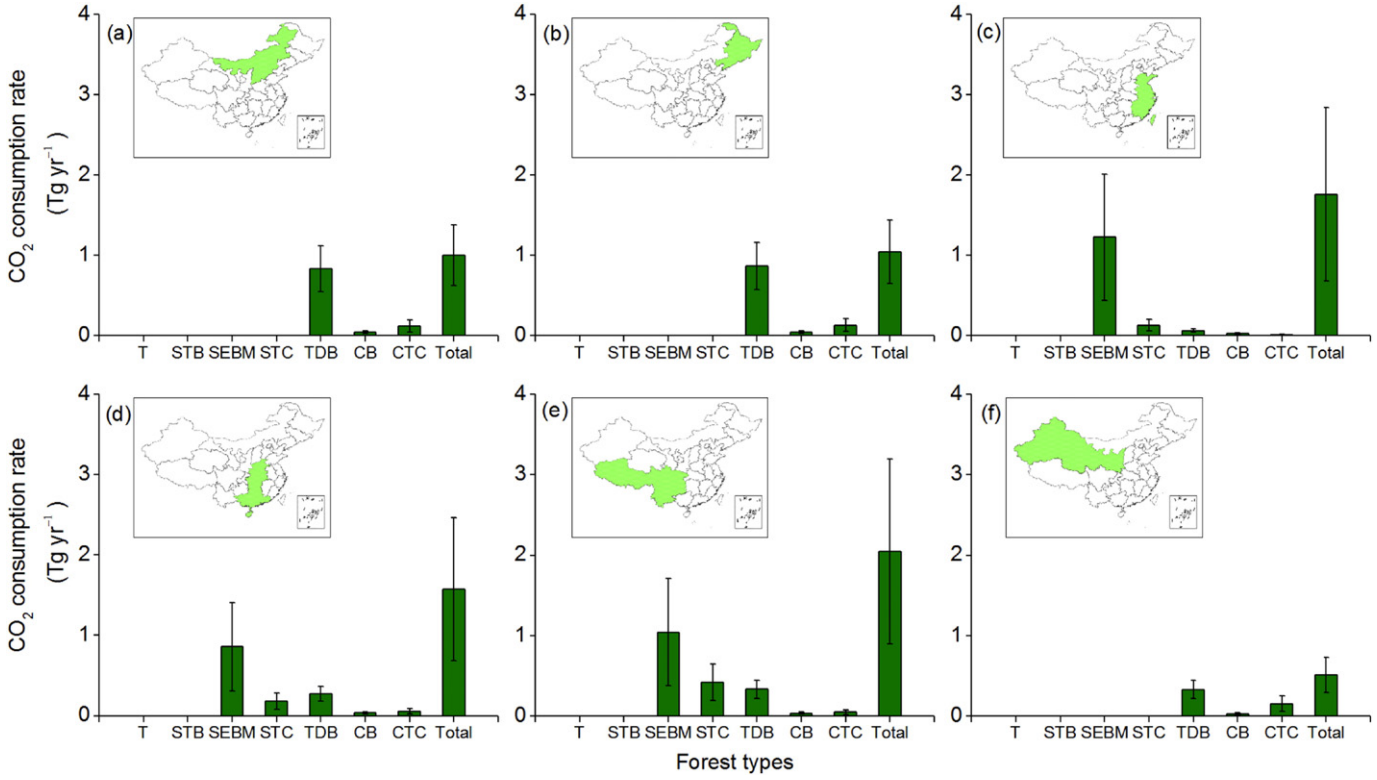

Fig. 4. The geographical distribution of CO_2 consumption rate by biomass-related silicate weathering ($R_{CO_2\ consumption,BSW}$, Tg CO_2 yr^{-1}) in different forest regions of China. (a) northern China; (b) northeastern China; (c) eastern China; (d) central southern China; (e) southwestern China; (f) northwestern China. *Total* = the sum of all the forests in the same region. The thin vertical bars represent standard deviations. For details on how CO_2 consumption rates were estimated see Materials and methods section.

weathering (with corresponding climate and vegetation) estimated via streamwater chemistry from Chinese watersheds (Li et al., 2016). The contribution of biomass-related weathering in other silicate-rich rock areas would be even greater due to more rapid weathering (Li et al., 2016). The potential CO_2 sequestration rate for biomass-related silicate weathering in China comprises approximately 34% of the traditional continental chemical weathering rate (Qiu et al., 2004; Wu et al., 2011).

To scale these calculations to a global level, it is important to consider the wide variation in NPP and biomass storage-harvest flux among the world's forests. The NPP of Earth's forests ranges from <2 t ha^{-1} yr^{-1} in boreal coniferous forests to >30 t ha^{-1} yr^{-1} in tropical evergreen broadleaf forests, with an average of 13.3 t ha^{-1} yr^{-1} (Pregitzer and Euskirchen, 2004). The total percentage of planted forests, and forests clearly impacted by anthropogenic activity globally (~70%) is much lower than that of Chinese forests (~90%) (Fang et al., 2001; FAO, 2010). It can be assumed that forests are less frequently harvested elsewhere in the world due to conservation practices. Using 30 ± 10% as the biomass harvest potential percentage of storage in forests globally (Vitousek et al., 1986; FAO, 2010), the biomass storage-harvest flux of the world's forests can be calculated as 3.9 ± 1.3 t ha^{-1} yr^{-1}. Assuming similar cation compositions to Chinese forests, the CO_2

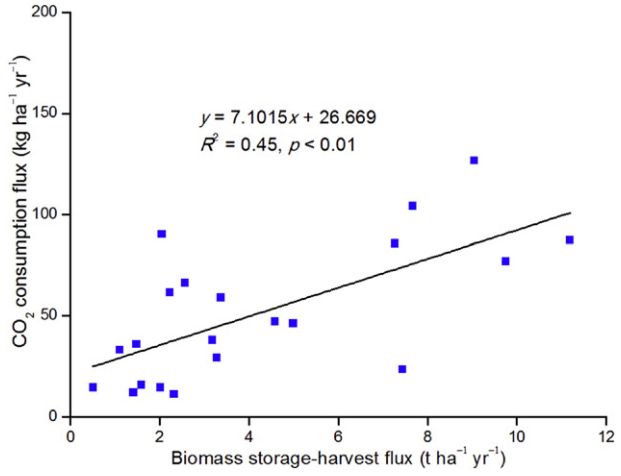

Fig. 5. Correlation of the CO_2 consumption flux by biomass-related silicate weathering ($F_{CO_2\ consumption,BSW}$, kg CO_2 ha^{-1} yr^{-1}) and the biomass storage-harvest flux ($F_{biomass,FBSH}$, t dry weight ha^{-1} yr^{-1}) for Chinese forests. Biomass storage-harvest flux was estimated from forest NPP; a forest biomass harvest potential percentage in storage of 40 ± 10% was used. For further details, see Materials and methods section.

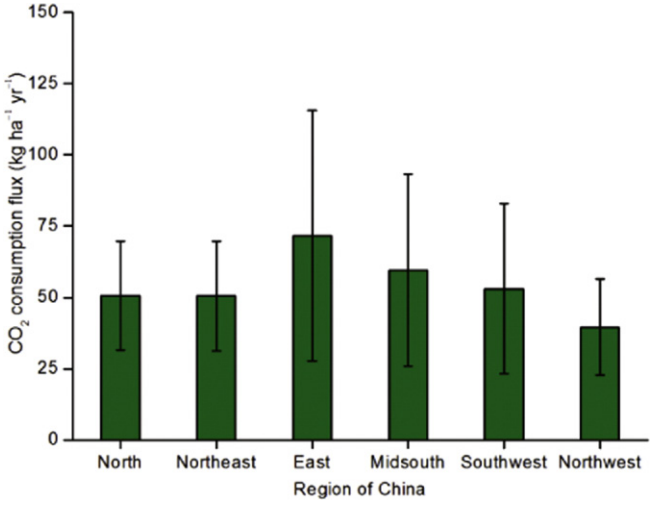

Fig. 6. CO_2 consumption flux of biomass-related silicate weathering ($F_{CO_2\ consumption,BSW}$, kg CO_2 ha^{-1} yr^{-1}) for different forest regions in China. CO_2 consumption flux of biomass-related silicate weathering was estimated using Eqs. (2)–(4). The thin vertical bars represent standard deviations.

consumption flux of biomass-related weathering globally is estimated to be 52 ± 14 kg CO_2 ha^{-1} yr^{-1}. The total area of the world's forests developed on soils dominated by silicate minerals is 4063 × 10^6 ha, approximately 2800 × 10^6 ha or 70% of which is affected with clearly visible human activity (FAO, 2010; Pan et al., 2011). Based on the area of the world's forests with clearly visible anthropogenic activity, we can estimate global CO_2 consumption rate from biomass-related silicate weathering. When biomass-related silicate weathering is combined with forest management practices such as silicate rock powder amendment in some forest regions with extremely acidic soils (Hartmann et al., 2013; Renforth et al., 2015; Taylor et al., 2016), it may strongly impact CO_2 sequestration. The potential global CO_2 consumption rate from biomass-related silicate weathering can reach 148 ± 40 Tg CO_2 yr^{-1}, and may contribute approximately 32% of the total from continental chemical weathering (Gaillardet et al., 1999). Further research is required to more accurately assess the potential global contribution. This includes determining site specific base cation mass balances for each forest, feedback of silicate weathering and biogeochemical base cation cycle, and efficiency of silicate rock powder amendment in base cation supply. Additionally, as the potential role of other vegetation types, notably grasslands in continental silicate weathering carbon sinks is should be further researched. Our study suggests that the CO_2 sequestration rate of continental silicate weathering at a millennial scale is underestimated using traditional methods (Gaillardet et al., 1999; Hagedorn and Cartwright, 2009; Beaulieu et al., 2012).

4.3. Sustainable forest management to increase biogeochemical C sequestration

The significant, potential global contribution (~32%) of forests to CO_2 sequestration by continental silicate weathering has crucial, practical implications. Firstly, it implies that the carbon sink of continental silicate weathering could be substantially increased by using scientifically-based forest management practices, such as afforestation/reforestation and planned forest harvesting. Secondly, these practices could further enhance CO_2 sequestration by focusing forest management on forest types that optimize CO_2 consumption flux, such as bamboo and other fast-growing forest plants (Fig. 3b). Empirical work in the subtropics of China has shown that afforestation/reforestation of bamboo forest can enhance CO_2 consumption flux of silicate weathering by 25% relative to that of other forest types (Song et al., 2011). Furthermore, because bamboo reaches maturity after 4–5 years, preferential harvesting of old bamboo every second year may help sustain the high NPP (Zhou et al., 2011), and hence the high CO_2 consumption flux of bamboo-enhanced silicate weathering. We project that 0.81 ± 0.49 Pg CO_2 could be stably sequestered through bamboo-enhanced silicate weathering over 100 years using a global potential area suited for bamboo cultivation of 100 × 10^6 ha (Zhou et al., 2011; Song et al., 2013) and the potential CO_2 consumption flux of 81 ± 49 kg CO_2 ha^{-1} yr^{-1} (Fig. 3b).

We therefore propose that the carbon sink of biomass-related silicate weathering, combined with other carbon sink mechanisms, such as weathering accelerated through addition of silicate rock powder (Köhler et al., 2010; Cressey, 2014), the accumulation of phytolith-occluded carbon (Parr et al., 2010; Song et al., 2013) and biomass organic carbon (the direct incorporation of CO_2 into the biomass) (Fang et al., 2001; Pan et al., 2011; Clemmensen et al., 2013) in forest ecosystems, could be comprehensively utilized to lower atmospheric CO_2 and mitigate global warming.

However, further studies such as response of base cation balance in forest soils, especially some acidified soils receiving significant atmospheric S and N deposition, to different forest harvest and silicate rock powder amendment technologies are required before the technology of biomass-related silicate weathering can be applied to sequester significant amounts of atmospheric CO_2 at a global scale.

5. Conclusions

We estimated the total potential CO_2 consumption rate for biomass-related silicate weathering in Chinese forests at 7.9 ± 4.1 Tg CO_2 yr^{-1}. Subtropical evergreen broad-leaf and mixed forest and temperate deciduous broad-leaf forest are the dominant contributors. The CO_2 consumption flux is significantly higher in angiosperm-dominated forest types (in particular, subtropical and tropical bamboo forest and subtropical evergreen broad-leaf and mixed forest) than in other forests. The carbon sink associated with continental silicate weathering could be substantially increased by using scientifically-based forest management practices, such as afforestation/reforestation and planned forest harvesting of bamboo and other fast-growing forest plants. This may be further enhanced when combined with other carbon sink mechanisms, such as accelerated weathering with supplementing with silicate rock powder. Future terrestrial biogeochemical C cycle models should seek to more explicitly incorporate biogeochemical silicate weathering modules.

Supplementary data to this article can be found online at https://doi.org/10.1016/j.scitotenv.2017.09.253.

Acknowledgements

We are grateful for support from the National Natural Science Foundation of China (41522207, 41571130042) and the State's Key Project of Research and Development Plan of China (2016YFA0601002). We thank the anonymous reviewers for their constructive comments. We thank Dr. Chongyang Xu for help in drawing Fig. 1.

The authors have declared no conflict of interest.

References

Amiotte-Suchet, P., Probst, J.L., Ludwig, W., 2003. Worldwide distribution of continental rock lithology: implications for the atmospheric/soil CO_2 uptake by continental weathering and alkalinity river transport to the oceans. Glob. Biogeochem. Cycles 17, 1038.

Balogh-Brunstad, Z., Keller, C.K., Bormann, B.T., O'Brien, R., Wang, D., Hawley, G., 2008. Chemical weathering and chemical denudation dynamics through ecosystem development and disturbance. Glob. Biogeochem. Cycles 22, GB1007.

Beaulieu, E., Goddéris, Y., Donnadieu, Y., Labat, D., 2012. High sensitivity of the continental-weathering carbon dioxide sink to future climate change. Nat. Clim. Chang. 2, 346–349.

Berner, R.A., 1997. The rise of plants and their effect on weathering and atmospheric CO_2. Science 276, 544–546.

Bormann, B.T., Wang, D., Snyder, M.C., Bormann, F.H., Benoit, G., April, R., Snyder, M.C., 1998. Rapid, plant-induced weathering in an aggrading experimental ecosystem. Biogeochemistry 43, 129–155.

Chen, L., Huang, J., Yan, C., 1997. Nutrient Cycles in Forest Ecosystems of China. Meteorology Press of China, Beijing, pp. 57–62.

Clemmensen, K.E., Bahr, A., Ovaskainen, O., Dahlberg, A., Ekblad, A., Wallander, H., Stenlid, J., Finlay, R.D., Wardle, D.A., Lindahl, B.D., 2013. Roots and associated fungi drive long-term carbon sequestration in boreal forest. Science 339, 1615–1618.

Cressey, D., 2014. Rock's power to mop up carbon revisited. Nature 505, 464.

Drever, J.I., 1994. The effect of land plants on the weathering rates of silicate minerals. Geochim. Cosmochim. Acta 58, 2325–2332.

Fang, J., Chen, A., Peng, C., Zhao, S., Ci, L., 2001. Changes in forest biomass carbon storage in China between 1949 and 1998. Science 292, 2320–2322.

Feng, Z., Wang, X., Wu, G., 1999. Biomass and Productivity of Forest Ecosystems in China. Science Press, Beijing, pp. 1–231.

Food and Agriculture Organization (FAO), 2010. Global Forest Resources Assessment 2010, Forestry Paper 163.

Futter, M.N., Klaminder, J., Lucas, R.W., Laudon, H., Köhler, S.J., 2012. Uncertainty in silicate mineral weathering rate estimates: source partitioning and policy implications. Environ. Res. Lett. 7, 024025.

Gaillardet, J., Dupré, B., Louvat, P., Allègre, C.J., 1999. Global silicate weathering and CO consumption rates deduced from the chemistry of large rivers. Chem. Geol. 159, 3–30.

Gislason, S.R., Oelkers, E.H., Eiriksdottir, E.S., Kardjilov, M.I., Gisladottir, G., Sigfusson, B., Snorrason, A., Elefsen, S., Hardardottir, J., Torssander, P., Oskarsson, N., 2009. Direct evidence of the feedback between climate and weathering. Earth Planet. Sci. Lett. 277, 213–222.

Hagedorn, B., Cartwright, I., 2009. Climatic and lithologic controls on the temporal and spatial variability of CO_2 consumption via chemical weathering: an example from the Australian Victorian Alps. Chem. Geol. 260, 234–253.

Hartmann, J., West, A.J., Renforth, P., Köhler, P., De La Rocha, C.L., Wolf-Gladrow, D.A., Dürr, H.H., Scheffran, J., 2013. Enhanced chemical weathering as a geoengineering strategy to reduce atmospheric carbon dioxide, supply nutrients, and mitigate ocean acidification. Rev. Geophys. 51 (2), 113–149.

Hou, X., 1982. Vegetation Geography of China and Chemical Composition of its Dominant Plants. Science Press, Beijing, pp. 188–243.
Huang, Z., Jiang, P., Song, Z., Meng, C., Wu, J., 2013. Uptake and accumulation characteristics of silicon and other nutritional elements in different age *Phyllostachys praecox* plants. Chin. J. Appl. Ecol. 24, 1347–1353 (in Chinese with English abstract).
Kardjilov, M.I., Gíslason, S.R., Gísladóttir, G., 2006. The effect of gross primary production, net primary production and net ecosystem exchange on the carbon fixation by chemical weathering of basalt in northeastern Iceland. J. Geochem. Explor. 88, 292–295.
Katagiri, S., Li, C., Nagayama, Y., Iwatsubo, G., 2005. Influences of human impact on nutrient cycling in deteriorated pine forests in Southern China. Jiangxi For. Sci. Tech. S1, 42–50 (in Chinese with English abstract).
Köhler, P., Hartmann, J., Wolf-Gladrow, D.A., 2010. Geoengineering potential of artificially enhanced silicate weathering of olivine. Proc. Natl. Acad. Sci. U. S. A. 107, 20228–20233.
Larsen, I.J., Almond, P.C., Eger, A., Stone, J.O., Montgomery, D.R., Malcolm, B., 2014. Rapid soil production and weathering in the Southern Alps, New Zealand. Science 343, 637–640.
Li, G., Ren, H., 2004. Biomass and net primary productivity of the forests in different climatic zones of China. Trop. Geogr. 24, 306–310 (in Chinese with English abstract).
Li, G., Hartmann, J., Derry, L.A., West, A.J., You, C.F., Long, X., Zhang, T., Li, L., Li, G., Qiu, W., Li, T., Liu, L., Chen, Y., Ji, J., Zhao, L., Chen, J., 2016. Temperature dependence of basalt weathering. Earth Planet. Sci. Lett. 443, 59–69.
Lucas, R.W., Holmström, H., Lämås, T., 2014. Intensive forest harvesting and pools of base cations in forest ecosystems: a modeling study using the Heureka decision support system. For. Ecol. Manag. 325, 26–36.
Ma, W., Li, Z., Ding, K., Huang, B., Nie, X., Lu, Y., Xiao, H., 2016. Soil erosion, organic carbon and nitrogen dynamics in planted forests: a case study in a hilly catchment of Hunan Province, China. Soil Tillage Res. 155, 69–77.
Maher, K., Chamberlain, C.P., 2014. Hydrologic regulation of chemical weathering and the geologic carbon cycle. Science 343, 1502–1504.
Manning, D.A., Renforth, P., 2012. Passive sequestration of atmospheric CO_2 through coupled plant-mineral reactions in urban soils. Environ. Sci. Technol. 47 (1), 135–141.
Manning, D.A.C., Renforth, P., Lopez-Capel, E., Robertson, S., Ghazireh, N., 2013. Carbonate precipitation in artificial soils produced from basaltic quarry fines and composts: an opportunity for passive carbon sequestration. Int. J. Greenhouse Gas Control 17, 309–317.
Meybeck, M., 1987. Global chemical weathering of surficial rocks estimated from river dissolved loads. Am. J. Sci. 287, 401–428.
Moosdorf, N., Renforth, P., Hartmann, J., 2014. Carbon dioxide efficiency of terrestrial enhanced weathering. Environ. Sci. Technol. 48 (9), 4809–4816.
Moulton, K.L., West, J., Berner, R.A., 2000. Solute flux and mineral mass balance approaches to the quantification of plant effects on silicate weathering. Am. J. Sci. 300, 539–570.
Pan, Y., Birdsey, R.A., Fang, J., Houghton, R., Kauppi, P.E., Kurz, W.A., Phillips, O.L., Shvidenko, A., Lewis, S.L., Canadell, J.G., Ciais, P., Jackson, R.B., Pacala, S.W., McGuire, A.D., Piao, S., Rautiainen, A., Sitch, S., Hayes, D., 2011. Large and persistent carbon sink in the world's forests. Science 333, 988–993.
Parr, J.F., Sullivan, L.A., Chen, B., Ye, G., 2010. Carbon bio-sequestration within the phytoliths of economic bamboo species. Glob. Chang. Biol. 16, 2661–2667.
Pregitzer, K.S., Euskirchen, E.S., 2004. Carbon cycling and storage in world forests: biome patterns related to forest age. Glob. Chang. Biol. 10, 2052–2077.
Qiu, D., Zhuang, D., Hu, Y., Yao, R., 2004. Estimation of carbon sink capacity caused by rock weathering in China. Earth Sci. 29, 177–183 (in Chinese with English abstract).
Renforth, P., von Strandmann, P.P., Henderson, G.M., 2015. The dissolution of olivine added to soil: implications for enhanced weathering. Appl. Geochem. 61, 109–118.
Schuiling, R.D., Krijgsman, P., 2006. Enhanced weathering: an effective and cheap tool to sequester CO_2. Clim. Chang. 74 (1−3), 349–354.
Song, Z., Zhao, S., Zhang, Y., Hu, G., Cao, Z., Wong, M., 2011. Plant impact on CO_2 consumption by silicate weathering: the role of bamboo. Bot. Rev. 77, 208–213.
Song, Z., Wang, H., Strong, P.J., Li, Z., Jiang, P., 2012. Plant impact on the coupled terrestrial biogeochemical cycles of silicon and carbon: implications to biogeochemical carbon sequestration. Earth-Sci. Rev. 115, 319–331.
Song, Z., Liu, H., Li, B., Yang, X., 2013. The production of phytolith-occluded carbon in Chinese forests: implications to biogeochemical carbon sequestration. Glob. Chang. Biol. 19, 2907–2915.
Street-Perrott, F.A., Barker, P.A., 2008. Biogenic silica: a neglected component of the coupled global continental biogeochemical cycles of carbon and silicon. Earth Surf. Process. Landf. 33, 1436–1457.
Sverdrup, H., Rosen, K., 1998. Long-term base cation mass balances for Swedish forests and the concept of sustainability. For. Ecol. Manag. 110 (1), 221–236.
Tang, J., Zhang, J., Song, Q., Huang, Z., Li, Z., Wang, L., Zeng, R., 2003. Biomass and net primary productivity of artificial tropical rainforest in Xishuangbanna. Chin. J. Appl. Ecol. 14, 1–6 (in Chinese with English abstract).
Taylor, L.L., Leake, J.R., Quirk, J., Hardy, K., Banwart, S.A., Beerling, D.J., 2009. Biological weathering and the long-term carbon cycle: integrating mycorrhizal evolution and function into the current paradigm. Geobiology 7, 171–191.
Taylor, L.L., Quirk, J., Thorley, R.M.S., Kharecha, P.A., Hansen, J., Ridgwell, A., Lomas, M.R., Banwart, S.A., Beerling, D.J., 2016. Enhanced weathering strategies for stabilizing climate and averting ocean acidification. Nat. Clim. Chang. 6, 402–406.
Uhlig, D., Schuessler, J.A., Bouchez, J., Dixon, J.L., von Blanckenburg, F., 2017. Quantifying nutrient uptake as driver of rock weathering in forest ecosystems by magnesium stable isotopes. Biogeosciences 14 (12), 3111.
Vadeboncoeur, M.A., Hamburg, S.P., Yanai, R.D., Blum, J.D., 2014. Rates of sustainable forest harvest depend on rotation length and weathering of soil minerals. For. Ecol. Manag. 318, 194–205.
Vitousek, P.M., Ehrlich, P.R., Ehrlich, A.H., Matson, P.A., 1986. Human appropriation of the products of photosynthesis. Bioscience 36, 368–373.
Wang, H., Xu, L., Sun, X., Lu, M., Du, X., Huo, Y., Snowball, I., 2011. Comparing mineral magnetic properties of sediments in two reservoirs in “strongly” and “mildly” eroded regions on the Guizhou Plateau, southwest China: a tool for inferring differences in sediment sources and soil erosion. Geomorphology 130, 255–271.
Wu, W., Zheng, H., Yang, J., Luo, C., Zhou, B., 2011. Chemical weathering of large river catchment in China and the global carbon cycle. Quat. Sci. 31, 397–408 (in Chinese with English abstract).
Zhang, H., Yu, D., Dong, L., Shi, X., Warner, E., Gu, Z., Sun, J., 2014. Regional soil erosion assessment from remote sensing data in rehabilitated high density canopy forests of southern China. Catena 123, 106–112.
Zhou, G., Meng, C., Jiang, P., Xu, Q., 2011. Review of carbon fixation in bamboo forests in China. Bot. Rev. 77, 262–270.